YTUP

Journal of Thermal Engineering
https://jten.yildiz.edu.tr/
https://doi.org/10.47481/jten.0027

RESEARCH ARTICLE

Experimental and 2D CFD study of thermoacoustic instabilities

Suchita K. Kadam[1,*], Nilaj N. Deshmukh[2]

[1]Ramrao Adik Institute of Technology, Nerul, Navi Mumbai 400706, India
[2]Department of Mechanical Engineering, Fr. C. Rodrigues Institute of Technology, Vashi, Navi Mumbai 400703, India

Abstract

Thermoacoustic instability, caused by the interaction of unsteady heat release and acoustic waves, is a significant challenge in combustion systems such as gas turbines and aero engines. To identify instability thresholds, this study investigates thermo-acoustic instability in a horizontal Rijke tube through experimental measurements and two-dimensional computational fluid dynamics (CFD) simulations. The study focuses on the effects of heat source positioning and boundary conditions, which are critical for optimising combustion system design. A heat source was placed at one-quarter of the tube's 800 mm length, and pressure oscillations were measured 150 mm from the heat source. Acoustic frequencies and sound pressure levels (SPL) were used to identify the instabilities. This study is unique in that it combines experimental and CFD approaches to systematically analyse the effects of heat source positioning and boundary conditions. The results show a strong agreement between experimental and simulated acoustic frequencies (216 Hz vs. 215 Hz), and the simulated values were set at a higher level to simplify the boundary condition. These results demonstrate the importance of accurate heat source positioning, appropriate specification of boundary conditions, and obtaining sufficient boundary-condition data. This study highlights the key mechanism related to the positioning of the heat source and the prescribed boundary condition in thermoacoustic instability. In addition, it proposes strategies to improve CFD models, reduce instabilities, and enhance the performance, efficiency, and safety of combustion systems.

Keywords: Thermoacoustic instability, rijke tube, experimental study, computational fluid dynamics (CFD), heat source positioning, acoustic frequencies

Cite this article as: Kadam, S. K., & Deshmukh, N. L. (2026). Experimental and 2D CFD study of thermoacoustic instabilities. Journal of Thermal Engineering, 12(4), 1243–1257. https://doi.org/10.47481/jten.0027

Highlights

The research examines thermoacoustic instability in a horizontal Rijke tube using experiments and CFD. The central factors affecting the instability thresholds and acoustic oscillations are examined. The principal observations of the study are:

- Thermoacoustic instability in a horizontal Rijke tube was investigated using experimental and CFD methods.
- The effect of heat source position and boundary conditions on instability was analysed.
- Strong agreement between experimental (216 Hz) and CFD (215 Hz) frequencies was observed.
- Higher SPL predicted in CFD is attributed to idealized boundary conditions and absence of damping.
- The study provides insights for improving combustion stability in gas turbines and aeroengines.

1. Introduction

Thermoacoustic instability arises when there are large variations in heat release that interact with acoustic waves to produce self-excited oscillations. This type of physical process has received notable attention from researchers because it produces detrimental effects on combustion systems, leading to pressure fluctuations that, in turn, increase the noise level and structural vibrations and, in severe cases, cause damage to the combustion chamber.

Lieuwen and Yang [1] reported that due to the mechanical wear of the components, the system will also fail because of the failure of connecting parts. They have conducted an in-depth analysis of the combustion instabilities in gas turbine engines, emphasizing the strong possibility of reduced performance.

*Corresponding Author
E-mail Adress: majid. suchita.kadam@rait.ac.in

Submitted: 1 December 2024 ; **Accepted:** 1 August 2025

This paper was recommended for publication in revised form by Editor-in-Chief Ahmet Selim Dalkılıç

After this Culick [2] studied irregular motions in combustion chambers which were not regular and pointed out their importance for power-generating systems and the corresponding risks.

According to Dowling and Mahmoudi [3], combustion noise is caused by the interaction between unsteady heat release and inherent acoustic modes in the system. Their results confirmed the Rayleigh criterion, which states that constructive interference between pressure oscillations and heat release fluctuations can strengthen them. Later, Dowling and Morgans [4] investigated feedback control strategies and its effect on thermoacoustic instability for reduce such kind of instabilities. They stated that the modification in phase relationship in between the heat release and acoustic pressure will be more effective Dowling and Stow [5] concluded in their study which was guided on premixed and partially premixed flame systems in most of the gas turbine combustors that the combustor geometry notably effect on the acoustic response and boundary condition also. Candel [6] analysed the problem which was due to combustion instabilities and formed the better understanding. He discussed the major issues that arose from dynamics and control of combustion instabilities.

For a very long time, researchers have used the Rijke tube as a standard experimental model to study combustion instability under well-controlled conditions, thereby reducing operational risks and hazards. Ducruix et al. [7] gave a theoretical framework for the following research work and showed the fundamental connection among acoustic pressure wave propagation and fluctuating heat release. The utilization of the Rijke tube in graphical modelling was described by Atis et al. [8]. When heat is introduced from within the Rijke tube, the air density inside it is changed and interacts with self-sustaining oscillations.

Johnson [9] studied the basic thresholds for the onset of amplitudes and the significance of temperature gradients on the excitation of pressure waves. Sarpotdar and Ananthkrishnan [10] have discussed mechanisms for feedback that keep Rijke tubes not stable after they have shed too much heat. Luo et al. [11] showed that the tube's motion could be changed with the tube shape and heat-source placement. Based on previous experiments, Deshmukh et al. [12] extended their research and showed that the pulsating radial micro-jet control system can effectively reduce instabilities in the horizontal Rijke tubes through external actuation.

Deshmukh, Kulkarni, and Ansari [13] constructed a design of a responsive passive Helmholtz resonator to reduce oscillations by actively changing the acoustic impedance. In a related study, an investigation of pointed and diffused air injection system and their effects on flame stability done by Deshmukh [14] illustrates the role of injector geometry and its effect on stability of the system. Overall, this study provides useful insights into the effects of normal orientation, burner configuration and boundary assumptions on thermally induced instability and indicates that the Rijke tube is a trustworthy platform for study of thermoacoustic instability. The experimental observations confirmed the theoretical results.

Deshmukh, Sharma, and Ansari [15] proposed a new method for the evaluation of temperature distribution along the lateral plane of the Rijke tube. This method provides a close analysis of the controlling instability. Rossetti, Candel, and Boeuf [16] studied the computational and experimental difficulties associated with industrial scale thermoacoustic instability, which highlights the importance of the Rijke tube investigations. Deshmukh et al. [17] investigated the effect of the tube length on oscillatory behaviour, and variation of heat input, which pointing out the impact of Helmholtz resonator geometry on reduction of suppression.

Signor, Shelton, and Majdalani [18] explored the spatially dispersed heat sources and their consequences on pressure wave patterns, which provide additional insights into the instability mechanism. From a computational perspective, Dang, Zhang, and Deguchi [19] examined the role of flames in generating instability and identified the key parameters responsible for flame suppression. Poinsot and Veynante [20] experimentally demonstrated the use of dispersed and focused air jets to control oscillations. Riaz and Stovall [21] verified and highlighted a relation between spatial heat release and acoustic feedback by using accuracy in computational fluid dynamics (CFD) models through the Rijke tube. Bhattacharya et al. [22] developed a very simple model for a two-source Rijke tube, showing the role of a passive control Helmholtz resonator that can reduce the acoustic energy, promoting stable combustion. Gövert et al. [23] implemented Large Eddy Simulations (LES) to adopt the complex physics of flow acoustic correlation in gas turbine combustors, and Dubey et al. [24] analysed the influence of mesh resolution, geometric configurations, and turbulence modelling on the prediction of instability behaviour. Lieuwen [25] developed the instruments that are used in simulation to manage instability and help to understand the effective design of the combustor.

Juniper and Sujith [26] explored the practical relevance of thermoacoustic research by examining the sensitivity and nonlinear behaviour in combustion systems. Goris [27] performed a numerical analysis to identify the important design factors that can increase the stability in horizontal combustors. Zhao and Nouri [28] suggested ways to diagnose problems that could make combustors less stable in different operating conditions. Cheng and Chen [29] examined the difference and variation in temporal behaviour of physical quantities like pressure, temperature and velocity through modelling and analysing thermoacoustic instabilities in aero engine combustors, and its dynamic behaviour.

Worth and Dawson [30] indicated from their study that the active control is necessary because the passive control method will not be enough to work alone, and it is required to control complex azimuthal modes that occur in an annular chamber. Emmert et al. [31] underscore the importance of the premixed flames in which the inherent instabilities may occur without any external force, so

this makes it very challenging to control by using passive control methods.

Silva [32] proposed combined methods for computer modelling and real-time optimization of combustor behaviour, but in practice, it proved difficult to implement on a real combustor due to the different types of fuel, complex geometries, and turbulence. This study indicates that further investigation is required to determine how the nonlinearities and the specific design affect thermoacoustic behaviour, also indicates that the hybrid system and real-time optimization type of development are the most efficient methods to control the instability, and this will be the most important direction for future research work.

Deshmukh et al. [12] studied the geometries of the horizontal Rijke tube using both CFD simulations and experiments. Their research mainly focused on specific control methods and limitations related to instability, rather than on boundary conditions, the location of the heat source, or differences in sound pressure level between simulation and experiment. Meanwhile, Dubey et al. [24] found that turbulence modelling and mesh resolution play a critical role in capturing thermoacoustic behaviour in CFD simulations.

In a vertically oriented classical Rijke tube, buoyancy-induced convection supports airflow within the hot part of the tube and promotes stronger coupling between unsteady heat release and acoustic waves. Horizontal Rijke tubes, on the other hand, dampen the effects of buoyancy by supporting airflow primarily through external means, such as fans. The horizontal orientation shows unique thermoacoustic characteristics, as the stability of oscillations is significantly affected by factors such as the heat-source location of the heat source, boundary conditions of the Rijke tube, and flow rate passing through the Rijke tube.

Furthermore, the development of different region inside the tube reach to the different temperature across the tube cross section that can change the acoustic energy inside the tube thereby influencing the operational stability limits of the system.

Horizontal Rijke tubes are considered more suitable and realistic for the modelling of actual combustion applications. Systems like gas turbines and aeroengines utilize horizontal orientation of the Rijke tube to enable the flow along the axis of the tube and optimized system design, as discussed by Lieuwen and Yang [1] and Dowling and Stow [5].

To mitigate these limitations, the present work adopts laboratory experimentation with 2-dimensional computational fluid dynamics analysis to examine the thermoacoustic instabilities in a horizontal Rijke tube. The research concentrates on the correlation between the acoustic oscillation and the heat release. This investigation is novel because it conducts detail comparison in numerical and experimental data to develop a complete understanding. These findings shed new light on how to improve instability control measures for both laboratory experiments and real-world combustion systems.

2. Experimental setup and methodology

The experimental setup, developed in a laboratory to investigate thermoacoustic instability in a Rijke tube, is shown in Figure 1 (schematic diagram) and Figure 2 (photographic views). In the experiment, a horizontal Rijke tube made of mild steel was used. The Rijke tube (length 800 mm, diameter 80 mm) had both ends open, and the burner was positioned 200 mm from one end of the tube. The tube was filled with LPG to ignite combustion in natural air, thereby generating thermoacoustic oscillations.

The position of the heat source was chosen in such a way that it favours the excitation of fundamental mode, which belongs to the low frequency oscillations in the tube. A blower was positioned towards the exit of the plenum chamber to achieve the uniform airflow within the plenum chamber and the Rijke tube. Combustion in the LPG-fuelled burner produced temperature differences in the low field that interacted with the airflow, generating acoustic oscillations and pressure variations. The microphone location was selected to correspond to the expected pressure node-antinode to capture the primary acoustic mode, and this location was 150 mm away from the open end of the Rijke tube to record the pressure variations

The analogue signals from the microphone were digitized using an NI-DAQ (National Instruments Data Acquisition System) and transferred to a computer for real-time monitoring, data storage, and analysis. The Fast Fourier Transform (FFT) method is able to convert a time-based signal to a frequency-based signal. This method was used to find the predominant frequencies when the oscillations settled into a regular pattern and reached a steady state. The setup allowed to study in detail the thermoacoustic instability by investigating the coupling within acoustic waves, pressure fluctuations and heat release in the system.

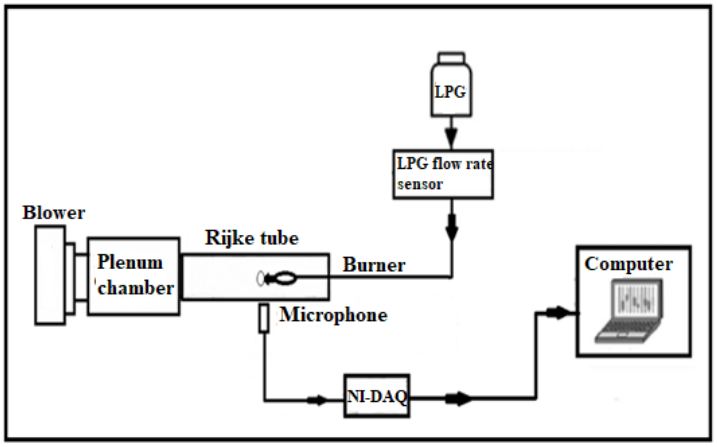

Figure 1. Illustration of the experimental setup used for thermoacoustic instability studies in a horizontal Rijke tube

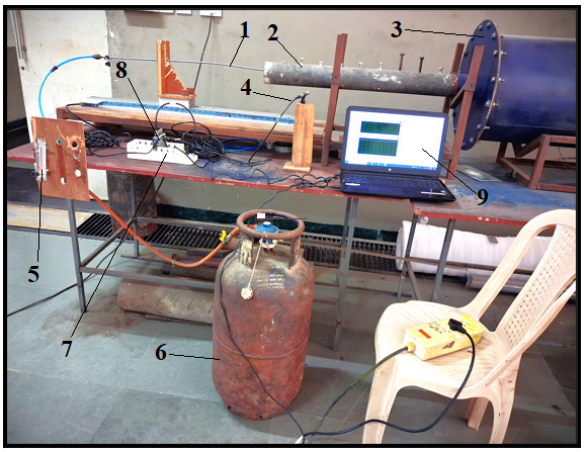

Figure 2. Photographic view of the thermoacoustic experimental arrangement

1. Burner tube	2. Rijke tube	3. Plenum chamber
4. Microphone	5. LPG flow rate sensor	6. LPG cylinder
7. NI cDAQ-9172	8. NI-9234	9. LabVIEW software

2.1. Instrumentation

2.1.1. Rijke tube

The Rijke tube is a hollow circular cylinder with an internal diameter of 80 mm and a length of approximately 800 mm. This cylinder is positioned horizontally, as shown in Figure 3, it is connected to the plenum chamber at one end, and the burner can be inserted at the other end.

Figure 3. Photographic view of the horizontal Rijke tube experimental setup

2.1.2. NI-DAQ

In this study, real-time data acquisition was performed using an eight-slot USB chassis (National Instruments' NI cDAQ-9172). This device is equipped with a C Series I/O module, which provides high accuracy in analogy and digital signal measurements and a high-speed USB connection, as shown in Figure 4. This system supports four channels of simultaneous analogy input with 24-bit resolution, to enable accurate sensor data collection. The specifications of the hardware used are given in Table 2.

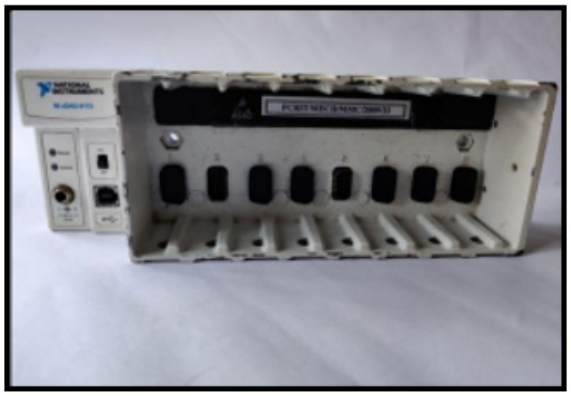

Figure 4. NI cDAQ-9172 data acquisition unit integrated with LabVIEW

Table 1. Specifications of the NI cDAQ-9172 data acquisition unit

Number of Channels	4 analogy input channels
ADC resolution	24 bits
Types of ADC	Delta-Sigma (with analogy pre-filtering)
Sampling mode	Simultaneous
Types of TEDS supported	IEEE 1451.4 TEDS Class I
Frequency	13.1072 MHz
Accuracy	±50 ppm maximum

2.1.3. NI-9234

The NI-9234 module, illustrated in Figure 5, is used to acquire sensor signals from accelerometers and proximity probes. The module provides four 24-bit-resolution analogy input channels, signal conditioning, and automatic filtering that depends on the sampling rate. The product is compatible with IEEE 1451.4 TEDS Class I and is used for sensor identification. It runs at 13.1072 MHz with an accuracy of ±50 ppm in measurement. The major specifications are tabulated in Table 3.

Figure 5. NI-9234 modular data acquisition system

Table 2. Key specifications of the NI-9234 data acquisition module

Number of Channels	4 analogy input channels
ADC resolution	24 bits
Types of ADC	Delta-Sigma (with analogy pre-filtering)
Sampling mode	Simultaneous
Types of TEDS supported	IEEE 1451.4 TEDS Class I
Frequency	13.1072 MHz
Accuracy	±50 ppm maximum

2.1.4. Microphone and preamplifier

The system utilizes an Onosokki condenser microphone (Figure 6) to measure sound pressure levels by translating air vibrations to electrical signals through changes in capacitance. It is functional in a frequency range of 10 Hz to 20 kHz and can be operated at sound pressure levels of up to 135 dB The microphone is operable with the MI-3111 preamplifier, which supports constant current operation (CCLD: 0.5 to 5 mA at 15–25 V) and delivers a maximum output voltage of 3 VRMS. It can be used in environmental conditions ranging from –10°C to +50°C and 25% to 90% relative humidity. Complete specifications are tabulated in Table 4.

Figure 6. Onosokki microphone Mi-1433 with preamplifier Mi-3111 used for acoustic measurements

Table 3. Technical specifications of the Onosokki condenser microphone and MI-3111 preamplifier

Frequency Range	10 Hz to 20 KHz
Operating Temperature Range	-10 To +50°C
Maximum Output Voltage	3 VRMS (With +15.0V Power Voltage)
Power Supply Voltage	CCLD (Constant Current Live Driver) 0.5 to 5mA/15 to 25V
Maximum Decibel Level	135 dB
Input Resistance	5G Ω ±15%
Operating Humidity Range	25% To 90 %Rh (Without Condensation)
Storage Temperature Range	-20°C to +60°C

2.1.5. LPG flow rate sensor

An Omron and their D6F-02L7-000 standard a sensor (Table 5) is used to measure the flow of LPG. The sensor provides stable measurements for flow rates ranging from 0 to 2 L/min. It features a Very quickly Joint P10 flow port and is LPG calibrated. The sensor is powered by 10.8 – 26.4 VDC, has a low current utilization of 15 mA and outputs 5.7 VDC. It offers accurate flow control with a precision of ±3% of the entire scale and has a three-pin standard connector for simple integration. It has a 5-bar burst atmospheric pressure rating and can operate with accuracy between –10°C and +60°C.

Table 4. Specifications of the Omron LPG Flow Sensor (D6F-02L7-000)

Manufacturer	Omron
Model no.	D6F-02L7-000
Flow rate range	0 – 2 L/min
Flow port type	Quick Joint P10
Calibration gas	LPG
Electrical connection	Three-pin connector
Power supply	10.8 to 26.4 Vdc
Current consumption	15mA max. with no load and Vcc of 12 to 24 VDC, GND = 0 Vdc, 25°C
Burst pressure	5 bars
Accuracy	± 3 % F.S.
Output voltage	5.7 Vdc
Operating temperature	-10 to +60°C

2.1.6. Measurement uncertainties

Uncertainties in the measurement instruments used in this research arise from multiple sources. Uncertainties in the Arduino Uno can be traced to environmental factors such as variations in power supply voltage and temperature changes, which are likely to affect microcontroller performance. Errors in measurements can occur in NI DAQ and NI9234 due to the analogue-to-digital conversion (ADC) process, in which the continuous signal is converted so that a computer can process it. These errors may be caused by temperature and voltage instability during measurement. Different types of microphones have different properties, which can influence the measurement fidelity of sound pressure level measurements. Accurate SPL measurement depends on the use of good and high-quality sensors in the microphone to obtain accurate SPL measurements and improve measurement accuracy.

The flow rate readings may vary within the range of ±3% Full Scale (F.S) accuracy with the Omron LPG Flow Rate Sensor and it was implemented with a measurement uncertainty. This suggests that measurement variations can be explained by limitations of the sensor quality and environmental parameters such as temperature and humidity. In addition to the above, some more uncertainties may also be present, such as variations in temperature, pressure, and power supply. These uncertainties occur inherently due to environmental factors and calibration. Therefore, while interpreting the results of the simulations and experiments, they should be considered.

3. Computational fluid dynamics modelling and simulation

This section presents the CFD modelling framework that was applied to the study of thermoacoustic instability in a horizontal Rijke tube. This includes all the governing equations, assumptions made during the basic simulations, and the boundary conditions.

3.1. Mathematical model

The mathematical model is derived from the Navier–Stokes equations, the acoustic wave equation, and the energy conservation principle; these equations represent the basic physical processes required to capture thermoacoustic instability.

Lieuwen and Yang [1] and Candel [6] present valuable insights and explain how the fluctuations in heat release interact with the acoustic pressure wave inside the combustion chamber. It also highlights the variation in the temperature gradient, which affects density and flow velocity and is responsible for coupling heat release and acoustic pressure. A deeper understanding of the fluctuations in acoustic pressure and unsteady heat release was done by Ducruix et al. [7] and Dowling and Mahmoudi [3], and its importance in accurate simulation to control the thermoacoustic behaviour.

3.1.1. Governing equations

Linearizing the continuity, momentum and energy equations gives the key equations describing acoustic waves and a normal reaction with a typical thermal addition in a Rijke tube. These equations are the relations between perturbations of pressure, density and velocity of the system. These perturbations are related to the heat addition rate by linearization of the energy equation. The pressure waves propagate through the tube and are governed by the acoustic wave equation, which is derived from the constant and momentum equations. At the open end of the tube the boundary conditions impose a zero-pressure perturbation. The natural frequencies and mode shapes of the resulting acoustic waves are determined by the boundary conditions.

1. Linearized continuity equation (conservation of mass):

   The continuity equation describes the relationship between the rate of change of density and the divergence of the velocity field. In its linearized form for small perturbations:

   Where, ρ' is the density fluctuation, ρ_0 is the mean density and u' is the velocity fluctuation. This formulation is foundational in combustion acoustics and is well-documented in studies on thermoacoustic instability (Lieuwen and Yang [1]; Culick [2]).

$$\frac{\partial \rho'}{\partial t} + \rho_0 \nabla \cdot u' = 0 \tag{1}$$

2. Linearized momentum equation: (conservation of momentum)

$$\frac{\partial u'}{\partial t} + \frac{1}{\rho_0} \nabla p' = 0 \tag{2}$$

   This equation governs the dynamics of the velocity field under the influence of pressure gradients where u' is the perturbation velocity (the deviation from the mean flow velocity, often referred to as the fluctuating velocity component),t is time, ρ0 is the reference or mean density of the fluid (in this case it is for air), p' is the pressure perturbation (the deviation from the mean pressure, often referred to as the fluctuating pressure component), ∇ is the gradient operator, which represents spatial derivatives in the x, y, and z directions, as discussed by Dowling and Mahmoudi [3].

3. Linearized energy equation: (conservation of energy)

$$\frac{\partial p'}{\partial t} - c_0^2 \frac{\partial p'}{\partial t} = \gamma \frac{q'}{V} \tag{3}$$

   This equation relates the changes in temperature and pressure perturbations to the rate of heat addition: where p' = Acoustic pressure fluctuation, t is Time, C_0 is Speed of sound in the medium, γ is Ratio of specific heats (Cp/Cv), q' is Heat release fluctuation and V is Volume, as discussed by Dowling and Morgans [4].

4. Acoustic wave equation:

$$\frac{\partial^2 p'}{\partial t^2} - c_0^2 \nabla^2 p' = 0 \tag{4}$$

   By combining the linearized continuity and momentum equations, we can derive the acoustic wave equation, which governs the propagation of pressure waves in the Rijke tube:

   In one dimension, for a tube of length L:

$$\frac{\partial^2 p'}{\partial t^2} - c_0^2 \frac{\partial^2 p'}{\partial x^2} = 0 \tag{5}$$

   Where, x is the spatial coordinate along the tube's length and p' is the pressure perturbation along the length of the tube as presented by Dowling and Stow [5].

5. Rayleigh criterion:
   The Rayleigh criterion provides the condition for the growth or decay of acoustic oscillations:

$$RI(x,t) = \frac{1}{T}\int_0^T p'(x,t)\, q'(x,t)\, dt > 0 \tag{6}$$

Where, RI(x, t) is the Rayleigh index at a given position x and time t, T is the period of oscillation, $p'(x, t)$ is the pressure perturbation at position x and time t and $q'(x, t)$ is the heat release rate perturbation at position x and time t, as elaborated by Candel [6]; Lieuwen and Yang [1].

The time-averaged product of pressure perturbations and heat-release-rate perturbations is positive. As a result, the oscillation amplitude will grow, leading to instability. To simplify the analysis, several common assumptions are made: To simplify the analysis, several common assumptions are applied:

1. All time-averaged properties of the airflow should remain constant along the length of the tube because adequate heat transfer occurs between the airflow and the tube wall.
2. Any hot air that passes over the heater inside the tube is rapidly cooled, so the air temperature remains near room temperature (300 K) throughout the process. This cooling effectively prevents the heater from exerting any considerable effect on the overall temperature rise. For most analysis purposes, the temperature can be considered constant.
3. This airflow removes most of the heat produced by the heater, transferring very little of it by radiation and conduction to other parts, such as the tube wall. The pressure drops along the length of the tube is also extremely low due to one-dimensional gas flow and the small amplitude of fluctuations.

3.2. Geometry of the rijke tube

In the experimental setup, a long mild steel tube with a length of 800 mm and a diameter of 80 mm was kept in a horizontal position. The same model was developed in the simulation. Figure 7 shows the two-dimensional geometry with the heat source located 200 mm away from the front end. In the simulation, the heat element was modelled as a thin disk positioned at one-quarter of the tube length, that is, 200 mm from the inlet. Figure 8 shows the axisymmetric geometry of the heat source. The reason behind selecting this position is that strong coupling between acoustic pressure and unsteady heat release was observed at this location, resulting in a pronounced acoustic response. This behaviour can be compared with the experimental results.

The tube is presumed to be axisymmetric, with both ends open for simplicity unless three-dimensional effects become important.

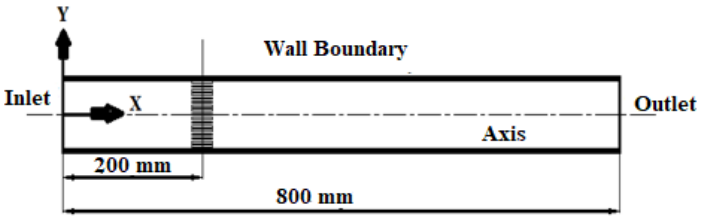

Figure 7. Illustrates the geometry of the Rijke tube along with its boundary conditions

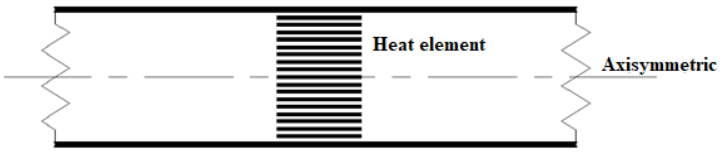

Figure 8. Axisymmetric representation of the heat source element

3.2.1 Meshing and boundary conditions

The linear theory predicts pressure oscillations and velocity perturbations, which can be captured by solving the discretized form of the linearized equations across the mesh. Variations in pressure and heat release rate can be used to assess the Rayleigh criterion at every mesh point. The computational domain is thus set up using meshing techniques to enable numerical solution of the governing equations, with the tube being divided into small elements or control volumes to allow solution via the finite element or finite volume method of the linearized equations. Mesh needs to be sufficiently fine, especially around the burner, as shown in Figure 9 (a) and (b) shows the magnified view of mesh refinement near the heat element because the pressure and velocity changes will be significant due to substantial heat addition.

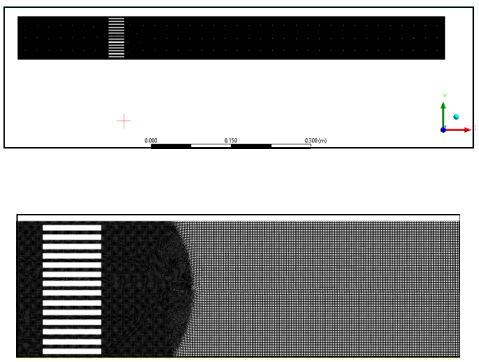

Figure 9. **(a)** Shows mesh distribution near the heating source. **(b)** Magnified view of the mesh refinement near the heat source

The boundary conditions at the open ends of the Rijke tube play a vital role in determining the system's behaviour. At these ends, the

pressure perturbation p′ is set to zero, representing the atmospheric pressure at the tube's openings, as stated by Juniper and Sujith [26].

In the equation below equation number 7 shows the conditions for the disturbance in pressure where it means x=0 and x=L which shows the end position of the tube

Equation 7 shows the boundary conditions for the pressure disturbances, where x = 0 and x = L represent the two end positions of the tube. The pressure variation, p′ , at the ends of the tube ensures the open boundary condition, where the pressure disturbance approaches zero [31]. The open boundaries at the ends of the tube remain exposed to the atmosphere, resulting in zero additional pressure disturbance.

a. Meanwhile, the velocity perturbations at the tube's ends are non-zero, allowing air movement and the propagation of acoustic waves. This arrangement guarantees that the waves are correctly reflected at the boundaries of the tube and that standing waves are formed.

3.2.2. Steady-state boundary conditions

In the Rijke tube steady state simulation, the system is defined with the boundary condition and solver parameters that are used to simulate the steady state behaviour of the circulation of air and heat transfer processes. The tube has an inlet rate of mass flow of 1.2×10-4 kg/s and the air is initially at 300 K, with the outlet open to the atmospheric pressure. The boundary conditions are depicted in Figure 10. The tube walls are adiabatic (no conductive heat transfer), and a "Symmetry" boundary condition is applied.

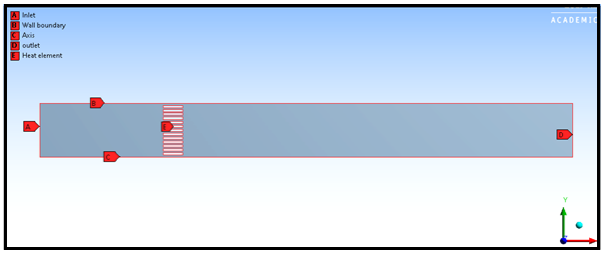

Figure 10. Representation of the boundary condition configuration for the two-dimensional computational model

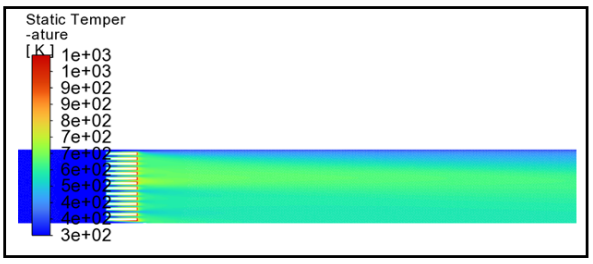

Figure 11. Heat variation near the heat element

The heater is kept at 300 K to create an idealized isothermal condition that simplifies the analysis of acoustic interactions, enabling the simulation to separate the effects of flow–acoustic coupling from those introduced by thermal gradients. The capacity to compress effects of the flow are handled using a pressure-based density solver and the energy-based equation is turned on to model the heat flow between the heating element and the airflow. Meshing is an important aspect and especially close to the heat origin region where severe gradients and normal boundary layers are observed. This is required for both steady-state and transient simulations. Figure 11 shows the temperature distribution around the heating element and Figure 12 shows an x-y plot of the variation of temperature around the heater.

The steady-state simulation results establish an independent baseline for analysing the onset of thermoacoustic instability. This baseline provides an essential foundation for subsequent transient turbulent simulations, in which the instability develops in accordance with the oscillations' time-dependent behaviour. Silva et al. [33] show that thermoacoustic feedback occurs, when unsteady heat release interacts with acoustic pressure waves. In this process, oscillations grow over time, leading to a feedback loop that results in resonance and combustion instability.

Furthermore, Balasubramanian and Sujith [34] explained that when the system becomes nonlinear, the response of the flame and flow does not remain proportional, and small disturbances may grow temporarily, playing a very important role in diffusion flame–acoustic interactions, also discussed about how important nonlinearity and non-normality are in diffusion flame–acoustic interactions. They said that when the system becomes nonlinear, the flame and flow do not respond proportionally, and small perturbations can undergo transient growth, which is highly relevant to diffusion flame–acoustic interactions.

These effects highlight the importance of choosing an appropriate solver and defining proper boundary conditions in the development of CFD models for the accurate representation of the characteristics of thermoacoustic instability.

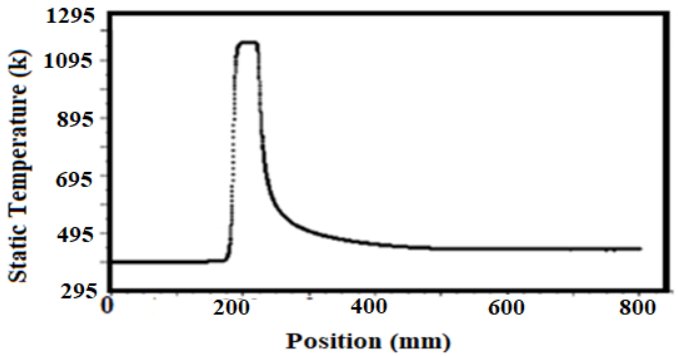

Figure 12. Depicts the temperature variation around the heating element

3.2.3. Transient state boundary conditions

In the "General" tab, the time-variant solver was selected. In the steady-state phase, the temperature of the heating elements was gradually increased from 300K to 1200K, as shown in Figure 12, to simulate heat input and provide the boundary condition for the turbulent flow. Then, in the "Boundary Condition" tab, the temperature for the heat elements is set to 1200K. In the "Solution Method" tab, "Second Order Implicit" was chosen to discretize the equations in time. In the "Surface Monitor" tab, outputs at a point were monitored over time steps. The receiver position is set at different positions on the Rijke tube wall to monitor the pressure-time data at those positions after the thermal elements, as indicated in the output reports. This stage is very time-consuming because the model oscillates within a very short period and so requires very small-time steps to capture it realistically. These small steps must then be repeated many, many times around 60,000 to 70,000 steps, until oscillations in the pressure become evident. The governing equations are then switched from laminar to turbulent flow regimes, and the K-ε model is employed. The result of this stage was the pressure difference over time at various points. At this stage, the problem was resolved.

3.2.4. Mesh independence study

Computational mesh independence analysis plays a very crucial role in confirming that the results of the CFD simulation will not change further when additional mesh refinement is performed. This approach improves the reliability and accuracy of the simulation, while also optimizing the computational cost and simulation time.

The grid-independence curve shown in Figure 13 illustrates how the amplitude changes as element size decreases. It shows that when fine meshing is applied to the model, the numerical solution becomes more stable. During the simulation, it was observed that when the element sizes of the meshing sets were between 0.008 mm and 0.001 mm, the amplitude increased from 202 Pa to 216 Pa, which indicates the numerical solution depends strongly on the grid refinement. Further refinement will not change the mesh. Table 6 shows the relationship among element size, number of elements number of nodes, and amplitude, which supports this observation.

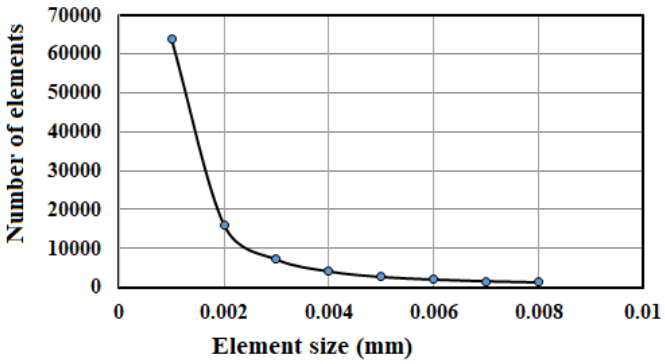

Figure 13. Illustrates the Mesh Independence Study

According to Polifke et al. [35], there will not be any longer significant effects on the flow behaviour and heat transfer after the refinement beyond a certain mesh density. Both studies show incremental refinement with stable values as the mesh level increases, and the grid independence analysis follows a smooth convergence trend.

The observed trend confirms that the adopted mesh maintains both computational efficiency and accurate numerical results. From Table 6, we can see that the results gradually converge with the improvement of the computational mesh quality, which indicates the importance of mesh sensitivity studies. When the results of the simulation are not changed with subsequent mesh improvement, the numerical estimations become more precise and reliable. The results of this study validate that the mesh refinement up to 216 Pa amplitude is accurate and no significant changes are seen with improved refinement compared to the selected mesh, ensuring a robust representation of the combustion instability behaviour. Such studies are important to ensure that the results of numerical simulations are accurate and that the actual physical behaviour is independent of mesh configuration.

Table 5. Grid Independence Test – Mesh Element Count for Different Element Sizes

Element Size (mm)	Number of Elements	Number of Nodes	Amplitude (pa)
0.001	63706	64752	216
0.002	16029	16540	214
0.003	7185	7525	212
0.004	4097	4360	210
0.005	2677	2881	208
0.006	2002	2174	206
0.007	1575	1760	204
0.008	1280	1470	202

4. Results and discussion

4.1. Experimental results

This experiment focused on measuring thermoacoustic pressure fluctuations. A microphone was placed at 150 mm from the horizontal Rijke tube. Variations in the pressure oscillations were measured with the microphone positioned downstream of the Rijke tube. The recorded acoustic pressure signals indicated the initiation and growth of self-sustained pressure fluctuations.

The time-history plot in Figure 14 shows the measured pressure signal, indicating that the flow behaviour is stable with very low-pressure oscillations. As the heater temperature increases, the pressure amplitude increases gradually and eventually exhibits periodic instability. An increase in amplitude indicates the importance of the coupling between acoustic pressure and heat release. The experimental results demonstrate the Rijke tube's natural behaviour,

including its natural frequency, and this behaviour is also confirmed by numerical simulation.

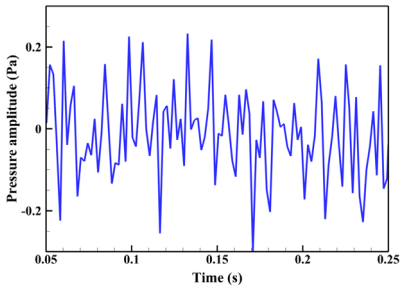

Figure 14. The experimental pressure disturbance recorded over time is shown

4.2. Transient simulation results

To capture the development of unsteady pressure behaviour in the horizontal Rijke tube, transient numerical simulations were performed. Pressure was measured at the same point as in the experiment (150 mm from the inlet) to facilitate comparison.

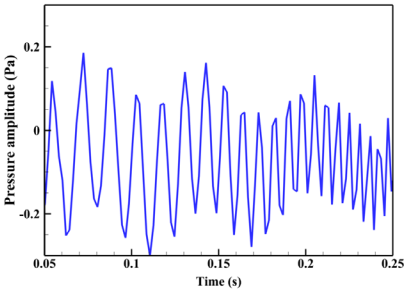

Figure 15. Simulated unsteady pressure disturbance over time

At the start of the experiment, the pressure fluctuations obtained from the simulation were recorded. Initially, these oscillations were small, and afterwards, they gradually grew with time. The initial response of the pressure oscillations is shown in Figure 15. The establishment of the stable limit cycle is shown in Figure 16, where the saturation of the pressure amplitude occurs because of acoustic feedback interactions.

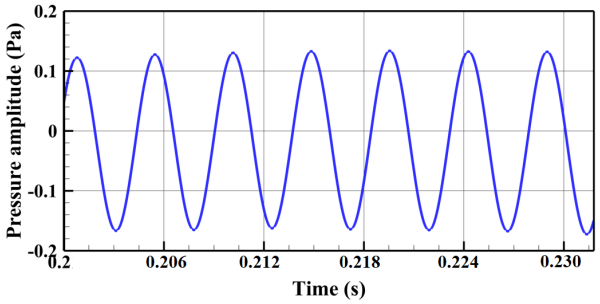

Figure 16. Time history of pressure oscillations depicting the onset and stabilization of limit cycle behaviour

4.3. Frequency analysis and higher harmonics

FFT analysis was performed on the simulated pressure data obtained from the computational simulation. Figure 17 shows the dominant frequency components observed in the simulation. Computational simulation was performed on a two-dimensional model in which both ends of the Rijke tube were kept open. The boundary conditions were idealized as atmospheric conditions, due to which the dominant fundamental frequency was observed to be 216 Hz, which is higher than the experimental frequency. In actual experimentation, several disturbances must be taken into consideration, such as reflection of acoustic waves, environmental disturbances, and end correction effects, which may influence the resonant frequency.

This deviation can be attributed to several factors:

- The 2D nature of the simulation, which reduces flow structures and underrepresents boundary layer effects.
- Numerical discretization that impacts the damping and thermal diffusion properties.
- The effect of higher acoustic modes was resolved in the computational model.

The presence of higher harmonics that are typical in the spectrum is an indication of complex acoustic interactions that are not easily captured by low-order models. These results show the ability of the simulation to capture fine wavelength details of thermal acoustic oscillations and enhance the experimental results.

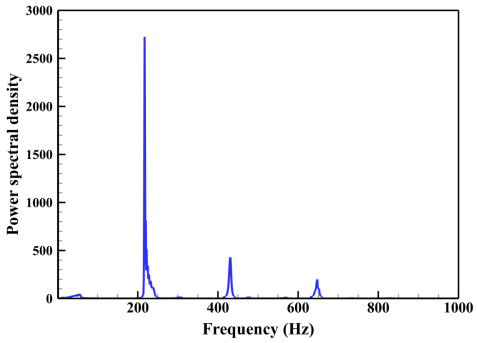

Figure 17. Frequency spectrum during the limit cycle regime

4.4. Validation of simulation results with experimental data

The reliability of the simulation was evaluated by comparing the predicted results with experimental measurements in terms of characteristic frequency and sound pressure level (SPL) of thermoacoustic oscillations.

Experimentally, the SPL was 95 dB (Figure 18b), whereas the simulation predicted a higher SPL of 127 dB (Figure 18a). This difference in SPL observed in the simulation can be attributed to multiple factors:

- Idealized Boundary Conditions: In a conventional physics simulation process, the wall surfaces of the Rijke tube are essentially stationary, expressing the acoustic energy rather than taking in it, keeping the waves of sound contained inside the tube. In actual experiments the noise waves travel via the tube, and a little of the sound power leaks out into the atmosphere so that the amplitudes of the oscillations decrease gradually because of energy decay in the system.
- Lack of Damping Mechanisms: In experimentation, the growth of the thermoacoustic oscillations becomes limited due to the many damping mechanisms naturally present to reduce the sound pressure level. Some examples of the damping effects are structural damping, thermal losses, and sound absorption by surrounding components. However, during CFD simulations, such types of damping mechanisms are not considered in the numerical model. The wall boundaries are assumed to be perfectly rigid, acoustically reflective, and with negligible energy losses. As a result, the acoustic energy stays longer, and therefore it leads to higher sound pressure predictions.
- Sensor Location and Signal Attenuation: In the simulation we measure acoustic pressure right next to the heat source, near a pressure antinode where the swings are naturally big. In the laboratory experimentation, the position of the microphone was kept at an approximate distance of 150 mm from the centre of the Rijke tube instead of positioning it near the flame region. As a result, the acoustic energy dissipates and spreads throughout the surrounding space. Due to this, the experimental SPL noted a lower sound pressure level than the CFD simulation.
- Dimensional Simplification (2D Effects): The two-dimension model cannot capture three-dimensional effects such as additional flow directions, vortical flow patterns, and normal radial energy losses, but it can record the essential relationship among the waves of sound and the flow. In real experimental Rijke tube combustors, mechanisms such as turbulent vortical structures, wall–fluid interactions, and secondary flow motion contribute to the natural dissipation of acoustic energy. As a result, the acoustic energy becomes weak, and the sound pressure level reduces. However, these damping and energy dissipation mechanisms are not fully represented in the 2D CFD model, due to which the acoustic energy remains trapped inside the Rijke tube, resulting in higher sound pressure level values compared to the experimental observations.
- Harmonic Content and Resonance Locking: In actual experimentation, due to noise disturbances and dissipation of acoustic energy, the higher-order harmonics become damped, as these harmonics are more likely to retain high acoustic energy during resonance locking.

The simulation also resolves additional modes and higher-order harmonics that may be damped during experimentation. With respect to frequency, the simulation showed a dominant acoustic mode at 216 Hz due to the assumption of idealized boundary conditions and the concentration of acoustic energy inside the Rijke tube, which resulted in the excitation of higher harmonic frequencies. In contrast, the experimental data were more concentrated around 215 Hz and exhibited fewer higher-order harmonics because several damping mechanisms caused sound energy attenuation and weakened the secondary peaks. The above comparison suggests that the CFD model overestimates the harmonic frequency content; however, the dominant instability frequency trends show close agreement with the experimental results.

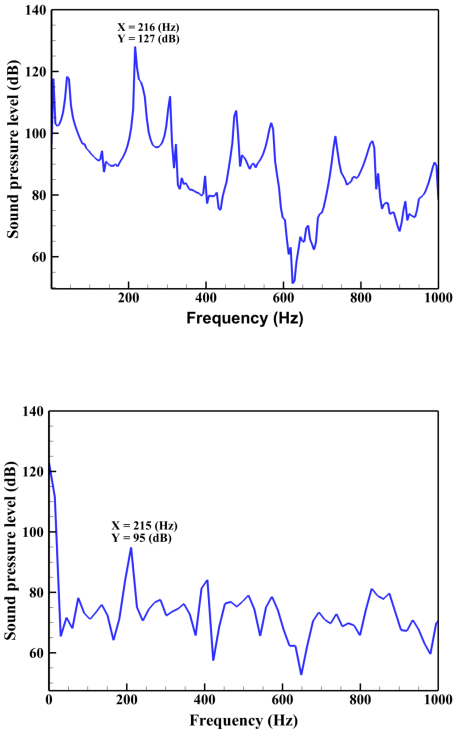

Figure 18. Frequency-domain SPL comparison: **(a)** CFD prediction, **(b)** Experimental data

4.5. Simulation uncertainties

One major source of uncertainty comes from the computational mesh resolution. If the mesh is too coarse, it can miss key flow structures, but making it finer raises the computational cost significantly. Simulation uncertainty also depends on the turbulence model chosen. Different models predict different swirl formation, flame behaviour and heat transfer, which affect the capturing of the development of unstable conditions and pressure oscillations. Additional uncertainties arise from the simple boundary conditions, the size of time step, the convergence criteria and the belief of two-dimensional flow. The environment-related outside variables like oscillations that occur due to variations in pressure and irregular temperature behaviour may affect the precision of the simulation. Other factors such as grid improvement and the choice of the time-step also affect the accuracy of the simulation. The incorrect estimation of the level of sound pressure is because of the lack of optimum damping

mechanism and the heat source simulation which may not be a good prediction of the actual heat-release behaviour.

4.6. Review and comparison of CFD studies on thermoacoustic instability

A comparative literature review has been carried out to critically analyse the scope and capabilities of existing CFD approaches for thermoacoustic instability in Rijke tubes. Primary research studies utilizing CFD methods to explore thermoacoustic effects in Rijke tubes between 2019 and 2024 are presented in the following table. The research work summarized in this table consists of approaches ranging from one-dimensional reduced-order modelling to detailed three-dimensional simulations. Each investigation is examined based on computational complexity, practical investigation focus, and its relevance to the present study. This evaluation helps identify the originality and applicability of the present work within the wider field of research.

Table 7. CFD-Based Studies on Thermoacoustic Instability in Rijke Tubes

Author (Year)	Rijke Tube Position	Study Focus	CFD Analysis	Relevance to Current Research
Dubey et al. (2019)	Vertical	Effect of geometrical parameters on instability	Yes (-)	Highlights geometry influence, supporting current study
Juniper & Sujith (2018)	Not applicable	Sensitivity and nonlinearity in thermoacoustic	No	Theoretical understanding complements current CFD
Zhao & Nouri (2019)	Not applicable	Thermoacoustic instability in industrial gas turbines	Yes (3D)	Validates industrial CFD modelling approaches
Cheng & Chen (2020)	Not applicable	Combustor instability analysis	Yes (-)	Supports use of CFD for combustor analysis
Bhattacharya et al. (2020)	Vertical	Reduced-order modelling of thermoacoustic instabilities	Yes (1D)	Offers simplified modelling contrast to current detailed CFD
Dang et al. (2021)	Vertical	Flame-induced thermoacoustic instability	Yes (2D)	Directly comparable to flame-induced instability studies
Beita et al. (2021)	Not applicable	High hydrogen combustion and instability	No	Supports background understanding, not direct CFD
Ayli et al. (2021)	Not applicable	Aero-acoustic study using FW-H equations	Yes (3D)	CFD technique insight; partially relevant
Luo et al. (2022)	Vertical	Experimental investigation on self-excited instability	Partial (mostly experimental)	Supports experimental methodology
Deshmukh et al. (2022)	Horizontal	Helmholtz resonator shape effect	Yes (2D)	Passive control method aligns with current suppression techniques
Silva (2023)	Not applicable	Intrinsic thermoacoustic instabilities	No	Theoretical background for instability types
Deshmukh et al. (2024)	Horizontal	Adaptive passive Helmholtz resonator for suppression	Yes (2D)	Highly relevant, exploring passive control strategies
Signor et al. (2024)	Vertical	Characterization of acoustic pressure waveforms	Yes (3D)	Complements CFD with advanced pressure analysis
Islam Rabby et al. (2025)	Not applicable	Nanofluids for energy savings (non-Rijke)	Yes (3D)	Not directly related, general CFD modelling insight

5. Conclusion and future work

To obtain a detailed understanding of thermoacoustic instability in a horizontal Rijke tube, the present study combines CFD simulations with experimental observations. While most earlier studies mainly focused on vertical Rijke tube configurations, the current work investigates thermoacoustic behaviour in a horizontal arrangement. In the horizontal orientation of the Rijke tube, the airflow inside the tube is mainly due to externally supplied airflow, which reduces the buoyancy effect that is usually strong in vertically positioned Rijke tubes. This behaviour represents a forced convection-dominant flow mechanism, resulting in thermoacoustic characteristics that differ from those observed in conventional vertical Rijke tube systems. This type of arrangement indicates the real design of combustion chamber found in aero-engines and gas turbines in which the horizontal position of the Rijke tube permit axial flow and optimized space. 216 Hz was the experimentally measured fundamental frequency, which shows close agreement with the 215 Hz CFD simulation frequency results. This shows that the CFD simulation and experimental results are able to record the primary acoustic mode.

A grid-independence analysis was carried out to confirm that all surface sections were sufficiently refined with a fine mesh, ensuring the reliability of the assumptions used in the CFD simulations. The findings of the present study highlight the importance of proper mesh refinement in accurately predicting thermoacoustic behaviour

and provide valuable insights for the design of efficient combustor systems.

In contrast, an observable variation was found in the SPL, where the CFD simulation showed 127 dB and the experimental results showed 95 dB. This was observed because the CFD analysis used perfectly defined boundary conditions and two-dimensional assumptions.

This study shows the effect of mesh resolution, the impact of the heat source location, and the treatment of boundary conditions on the management of thermoacoustic instability. The close agreement in frequency results demonstrates that ideal two-dimensional CFD models can be effectively used for preliminary design analysis.

On the other hand, previous studies have shown that the advantages of using three-dimensional CFD modelling are its capability to reduce the excessive prediction of SPL values and provide more realistic damping effects.

For designing the most efficient combustor system, this study provides useful information that helps to examine the burner location, proper arrangement of the system, and flow conditions that can affect thermoacoustic behaviour and achieve better combustion performance. These important findings play a role in the development of more stable and optimized combustion systems.

The interaction that occurs between release of heat and pressure acoustic fluctuations can be controlled in order to minimize thermoacoustic instability. The results presented here can be useful for engineers to design stable and significantly capable the combustion process systems for practical applications.

Key Findings:

- Based on the experimentation, the fundamental governing frequency corresponding to 216 Hz was noticed which allows one to evaluate the temperature-dependent instability in the horizontal Rijke tube.
- The measured sound pressure level was 95 dB in the experiment and the approximated result from the CFD simulation was 127 dB. The difference in the predicted value of sound pressure level came from the imaginary boundary assumptions and the difficulties in two-dimensional modelling.
- The simulated frequency spectrum revealed a dominant peak at 216 Hz with higher harmonics, while the experimental spectrum's energy was centred at 215 Hz.
- This study mainly focused on horizontal position of the Rijke tube which enhances the detailed valuable insights of the thermoacoustic instability behaviour
- Highlighting the horizontal configuration is the main objective of this study which offers fresh perspectives into the thermally coupled acoustic mechanisms that are essential in the combustion process system.
- The extracted results can be validated and compared with earlier investigations, that offers most useful insights to identify the complex acoustic modes and harmonic responses. Further investigations can enhance and improve the accuracy of CFD simulations through sophisticated simulation methods and improved numerical frameworks.
- Extending present 2D simulations into a 3D framework will enable them to describe complicated flow patterns, acoustic phenomena, and turbulence more accurately.
- More advanced simulations such as the improved Reynolds-Averaged Navier-Stokes (RANS) and Large Eddy Simulation (LES) are applied to resolve the complicated turbulent flow structures that conventional models for turbulence are not able to. Such models can thus be used in future studies.

Realistic boundary conditions such as friction-related losses, inefficient heat conduction, wall-based interactions, damping mechanisms can be applied to reduce the deviation between numerical and currently experimental standard sound pressure level (SPL) values.

Factors such as imperfect heat conduction through the walls, friction losses, detailed wall-fluid interactions, and acoustic attenuation mechanisms can be integrated to reduce the differences between experimental and numerical results. This can improve the accuracy of CFD simulations and provide a more realistic representation of thermoacoustic behaviour.

In CFD simulations most parameters are given in advance. If realistic boundary conditions are however considered, the accuracy of the simulation can be improved. Friction loss, imperfect temperature transfer through the walls, detailed interaction between the walls and the fluid, and realistic acoustic adsorption mechanisms may all be introduced to diminish the discrepancies between the numerical and experimental results.

Studies examining the effects of various burner positions, tube geometry, heat-input oscillations, and combustion-system aspect ratios can help identify conditions that enhance suppression of thermoacoustic instability.

Artificial intelligence (AI) and machine learning (ML) methods can be used to provide more realistic predictions and to obtain better control over thermoacoustic instability. Future research in this area could support the development of active control strategies.

Nomenclature

CFD	Computational Fluid Dynamics
SPL	Sound Pressure Level, usually measured in deci bels (dB)
zu	Velocity in the axial direction, measured in meters per second (m/s)

v	Velocity in the radial direction, measured in meters per second (m/s)
ρ	Fluid density, measured in kilograms per cubic meter (kg/m³)
μ	Dynamic viscosity, measured in Pascal-seconds (Pa*s)
k	Turbulent kinetic energy or thermal conductivity, depending on context
ν	Kinematic viscosity, measured in square meters per second (m²/s)
p	Static pressure, measured in Pascal's (Pa)
T	Temperature, measured in kelvin (K)
Q	Heat release rate, measured in watts (W)
f	Frequency, measured in hertz (Hz)
ANSYS	Commercial CFD software used for simulation
FFT	Fast Fourier Transform, used for frequency do main analysis
L	Length of the Rijke tube, measured in millimetres (mm)
D	Diameter of the Rijke tube, measured in millimetres (mm)
LPG	Liquefied Petroleum Gas
NI-DAQ	National Instruments Data Acquisition System

References

[1] T. Lieuwen and V. Yang, Combustion Instabilities in Gas Turbine Engines: Operational Experience, Fundamental Mechanisms, and Modelling. Reston, VA, USA: AIAA, 2005. doi: 10.2514/4.866807.

[2] F. E. C. Culick, Unsteady Motions in Combustion Chambers for Propulsion Systems. Neuilly-sur-Seine, France: NATO Research and Technology Organization, 2006.

[3] A. P. Dowling and Y. Mahmoudi, "Combustion noise," Proc. Combust. Inst., vol. 35, no. 1, pp. 65–100, 2015, doi: 10.1016/j.proci.2014.08.016.

[4] A. P. Dowling and A. S. Morgans, "Feedback control of combustion oscillations," Annu. Rev. Fluid Mech., vol. 37, pp. 151–182, 2005, doi: 10.1146/annurev.fluid.36.050802.122038.

[5] A. P. Dowling and S. R. Stow, "Acoustic analysis of gas turbine combustors," J. Propuls. Power, vol. 28, no. 5, pp. 751–764, 2012, doi: 10.2514/2.6192.

[6] S. Candel, "Combustion dynamics and control: progress and challenges," Proc. Combust. Inst., vol. 29, no. 1, pp. 1–28, 2002, doi: 10.1016/S1540-7489(02)80007-4.

[7] S. Ducruix, S. Candel, D. Durox, and T. Schuller, "Combustion dynamics and instabilities: elementary coupling and driving mechanisms," J. Propuls. Power, vol. 19, no. 5, pp. 722–734, 2003, doi: 10.2514/2.6182.

[8] C. A. A. Atis, M. Sarker, and M. Ehsan, "Study of thermoacoustic phenomenon in a Rijke tube," Procedia Eng., vol. 90, pp. 589–594, 2014, doi: 10.1016/j.proeng.2014.11.774.

[9] J. T. Johnson, "Experiments on the Rijke-tube phenomenon," J. Acoust. Soc. Am., vol. 36, no. 9, pp. 1737–1742, 1964, doi: 10.1121/1.1919275.

[10] S. Sarpotdar and S. Ananthkrishnan, "The Rijke tube – A thermoacoustic device," Resonance, vol. 8, no. 1, pp. 59–71, 2003, doi: 10.1007/BF02834451.

[11] L. Luo, T. Li, J. Deng, R. Zhao, J. Wang, and L. Xu, "Experimental investigation on self-excited thermoacoustic instability in a Rijke tube," Appl. Sci., vol. 12, no. 16, p. 8046, 2022, doi: 10.3390/app12168046.

[12] N. N. Deshmukh et al., "Suppression of thermoacoustic instabilities in horizontal Rijke tube using pulsating radial jets," MethodsX, vol. 11, p. 102325, Aug. 2023, doi: 10.1016/j.mex.2023.102325.

[13] N. N. Deshmukh, A. Kulkarni, and A. Ansari, "Suppression of thermoacoustic instability inside a Rijke tube using an adaptive passive Helmholtz resonator," J. Inst. Eng. India Ser. C, vol. 105, no. 3, pp. 345–352, 2024, doi: 10.1007/s40032-024-01050-

[14] N. N. Deshmukh, "Effect of pointed and diffused air injection on premixed flame confined in a Rijke tube," Cogent Eng., vol. 3, no. 1, p. 1156280, 2016, doi: 10.1080/23311916.2016.1156280.

[15] N. N. Deshmukh, S. D. Sharma, and A. F. Ansari, "Experimental method for temperature measurement on lateral planes along a Rijke tube to assess efficacy of control method," MethodsX, vol. 10, p. 102170, 2023, doi: 10.1016/j.mex.2023.102170.

[16] G. F. Rossetti, F. Candel, and P. Boeuf, "Thermoacoustic instabilities in industrial burners: A review of experimental and computational challenges," Prog. Energy Combust. Sci., vol. 45, pp. 1–30, 2015, doi: 10.1016/j.pecs.2014.08.001.

[17] N. N. Deshmukh et al., "Effect of Helmholtz resonator shape on suppression of thermoacoustic instability," IOP Conf. Ser. Mater. Sci. Eng., vol. 1259, no. 1, p. 012002, 2022, doi: 10.1088/1757-899X/1259/1/012002.

[18] E. T. Signor, C. M. Shelton, and J. Majdalani, "Characterization of the acoustic pressure waveforms in Rijke tubes with spatially varying heat sources and temperature distributions," Phys. Fluids, vol. 36, no. 3, p. 034113, 2024, doi: 10.1063/5.0194337.

[19] N. Dang, J. Zhang, and Y. Deguchi, "Numerical study on the route of flame-induced thermoacoustic instability in a Rijke burner," Appl. Sci., vol. 11, no. 4, p. 1590, Feb. 2021, doi: 10.3390/app11041590.

[20] T. Poinsot and S. Veynante, Theoretical and Numerical Combustion. Cambridge, UK: Cambridge University Press, 2012.

[21] M. A. Riaz and T. B. G. Stovall, "Validation of CFD simulations for thermoacoustic instability in a Rijke tube," J. Fluid Mech., vol. 755, pp. 432–456, 2014.

[22] C. Bhattacharya, S. Mondal, A. Ray, and A. Mukhopadhyay, "Reduced-order modelling of thermoacoustic instabilities in a two-heater Rijke tube," Combust. Theory Model., vol. 24, no. 3, pp. 530–548, 2020, doi: 10.1080/13647830.2020.1714080.

[23] S. Gövert, J. T. Lipkowicz, B. Janus, and R. C. S. Evans, "Large eddy simulation of thermoacoustic oscillations in gas turbines," J. Eng. Gas Turbines Power, vol. 146, no. 1, p. 011011, Jan. 2024, doi: 10.1115/1.4063419.

[24] A. K. Dubey, K. Yoichiro, H. Nozomu, and F. Osamu, "Effect of geometrical parameters on thermoacoustic instability of downward propagating flames in tubes," Proc. Combust. Inst., vol. 37, no. 2, pp. 1869–1877, 2019, doi: 10.1016/j.proci.2018.06.155.

[25] T. Lieuwen, "Modelling premixed combustion-acoustic wave interactions: A review," J. Propuls. Power, vol. 19, pp. 765–781, 2003, doi: 10.2514/2.6193.

[26] M. P. Juniper and R. I. Sujith, "Sensitivity and nonlinearity of thermoacoustic oscillations," Annu. Rev. Fluid Mech., vol. 50, pp. 661–689, 2018, doi: 10.1146/annurev-fluid-122316-045125.

[27] W. W. M. M. Goris, "Numerical investigation of thermoacoustic instabilities in horizontal combustors," Int. J. Heat Fluid Flow, vol. 45, pp. 224–238, 2014.

[28] G. Zhao and M. Nouri, "Analysis of thermoacoustic instability in industrial gas turbines," J. Propuls. Power, vol. 35, no. 4, pp. 1074–1085, 2019, doi: 10.2514/1.B36663.

[29] J. Cheng and H. Chen, "Modelling and analysis of thermoacoustic instability in aero-engine combustors," Aerosp. Sci. Technol., vol. 98, p. 105708, 2020, doi: 10.1016/j.ast.2020.105708.

[30] N. A. Worth and J. R. Dawson, "Modal dynamics of self-excited azimuthal instabilities in an annular combustion chamber," Combust. Flame, vol. 160, no. 11, pp. 2476–2489, 2013, doi: 10.1016/j.combustflame.2013.04.031.

[31] T. Emmert, S. Bomberg, and W. Polifke, "Intrinsic thermoacoustic instability of premixed flames," Combust. Flame, vol. 162, no. 1, pp. 75–85, 2015, doi: 10.1016/j.combustflame.2014.06.008.

[32] C. F. Silva, "Intrinsic thermoacoustic instabilities," Prog. Energy Combust. Sci., vol. 95, p. 101065, 2023, doi: 10.1016/j.pecs.2022.101065.

[33] C. F. Silva, M. Merk, T. Komarek, and W. Polifke, "The contribution of intrinsic thermoacoustic feedback to combustion noise and resonances of a confined turbulent premixed flame," Combustion and Flame, vol. 182, pp. 269–278, Aug. 2017, doi: 10.1016/j.combustflame.2017.04.015.

[34] K. Balasubramanian and R. Sujith, "Non-normality and nonlinearity in combustion–acoustic interaction in diffusion flames – CORRIGENDUM," Journal of Fluid Mechanics, vol. 733, p. 680, Oct. 2013, doi: 10.1017/jfm.2013.411.

[35] W. Polifke, A. Poncet, C. O. Paschereit, and K. Döbbeling, "Reconstruction of acoustic transfer matrices by instationary computational fluid dynamics," Journal of Sound and Vibration, vol. 245, no. 3, pp. 483–510, 2001, doi: 10.1006/jsvi.2001.3594.